Lasers in Manufacturing Conference 2021

Predicting qualitative and quantitative properties of metal powders for additive generative manufacturing using hyperspectral imaging and machine learning

Florian Gruber[a], Christoph Wilsnack[a], Axel Marquardt[a,b], Julius Hendl[a,b], Sebastian Witte[a,c], Martin Schäfer [d,*], Karol Kozak[a,b,c], Wulf Grählert[a], Lukas Stepien[a]

[a]*Fraunhofer IWS, Winterbergstraße 28, 01277 Dresden, Germany*
[b]*Technische Universität Dresden, Helmholtzstraße 7, 01069 Dresden, Germany*
[C]*Institut für Angewandte Informatik, Goerdelering 9, 04109 Leipzig, Germany*
[d]*Siemens AG Technology; Siemensdamm 50, 13629 Berlin*

Abstract

Quality control of metal powders in powder bed-based additive manufacturing processes is currently very time-consuming and costly and is not possible inline, i.e. during the process. The powder properties are of crucial importance for the quality of the components produced. A fast and complete inline characterization of metal powders is therefore desirable. In this work, a method for powder quality control based on hyperspectral imaging and machine learning is presented. The aim is to qualitatively distinguish different powder types and powder charges based on hyperspectral measurements, and to quantitatively predict some powder properties (size distribution and sphericity). The determination of powder type and charge was possible for the investigated samples with an accuracy of up to 100 %, and good results were also achieved for the quantitative prediction of powder properties. The results show that hyperspectral imaging appears to be a promising method for inline powder characterization for additive manufacturing processes.

Keywords: additive manufacturing; powder characterization; hyperspectral imaging; machine learning

1. Introduction

Additive Manufacturing (AM) emerged in the last decade from a method for rapid prototyping to a promising candidate for the manufacturing of fully functional complex parts in serial production. A main challenge of the integration of AM into already established industrial process chains is caused by the still

* Corresponding author.
E-mail address: martin.schaefer@siemens.com .

limited standardization and a not fully established quality assurance along the process chain. This is a major topic in the industrialization process of AM (Steven et al. 2020).

As a starting point of the process chain often, the feedstock procurement for the processes is a major topic of the material related quality assurance. This is especially true for metal powder-based AM processes like the Laser Powder Bed Fusion (LPBF) or LMD (Laser Metal Deposition). The focus of the quality assurance of metal powders for AM lies on common powder characterization methods for the assessment of the morphology, the chemistry and the rheology. Quality control of metal powders for AM is a time-consuming and cost-intensive process. In particular, AM processes in which the residual powder is reused, such as powder bed-based processes, require intensive monitoring of the powder quality. This is the key to identifying unwanted changes in powder quality due to oxidation, segregation and contamination, and to avoid impacts on the quality of the produced parts. Therefore, key performance indicators and new technologies for fast powder quality screening need to be identified, evaluated and established.

Hyper Spectral Imaging (HSI) is a promising method for the detection of qualitative and quantitative changes of powders. HSI allows the spatial and spectral properties of metal powders to be measured with high resolution and is therefore ideally suited for detecting chemical and morphological changes in the powders. Initial investigations have shown that it is possible, for example, to determine the degree of deterioration of various powder samples with high accuracy (Linaschke et al. 2019). Based on these results, the present paper describes the further development of this approach.

Therefore, a large amount of powder samples from different stages of the powder life cycle were collected and characterized with the common powder characterization methods and measured with two HSI setups in the visible and near-infrared (VNIR) spectral range. The collected data was then used to train, optimize and validate machine learning models for the prediction of powder properties from the hyperspectral measurements of the powders. The powder properties considered are the size distribution of the powders and their sphericity. In addition, it was tried to distinguish two different powder materials, as well as two batches of the same powder material. This could enable a novel and fast screening method for the quality assurance of metal powders for AM.

2. Materials and methods

2.1. Powder sample preparation

The powders investigated in the project are one batch of the steel material 316L (1.4404) and two batches of the nickel-based alloy Inconel718 (2.4668). The 1st batch of the Inconel 718 consists of 25 samples and each sample was measured before and after sieving. The 2nd batch contains 10 samples for each sieving condition. For the 316L powder 14 samples for each sieving condition were measured.

Both materials are two powders currently frequently used in industry in the laser melting process. Both their application possibilities, the processability in the process and the already defined material properties of the AM material result in this industrial use.

316L describes stainless, austenitic chromium-nickel-molybdenum steels, which have good resistance in non-oxidizing acids and chlorine-containing media. Due to its chemical composition, the material is a corrosion-resistant metal alloy. 316L differs from 316 in that it has lower carbon content.

Due to its good heat-resistant properties (corrosion resistance; high tensile, fatigue, creep and fracture strength up to 700°C), the nickel alloy Inconel718 is increasingly used in energy technology (e.g., exhaust gas components in gas turbine construction), the oil and gas industry, aerospace and racing. The grain size distribution is generally used in the range of 15 to 45 µm for laser melting systems. The best possible spherical particle shape and powder flowability for the respective equipment should be achieved.

To obtain measurement data that is as realistic as possible powder samples were taken at regular base from ongoing production operations after each building process. The systems used for the processing are laser melting systems from the companies EOS (EOS M 290, EOS GmbH, Krailling, Germany) and SLM Solutions (SLM 280, SLM Solutions Group AG, Lübeck, Germany). To include the influence of the sieving of the powder before reuse in the sampling, the powder samples were taken in the construction space and after sieving. The powder samples were collected in two ways: On the one hand, containers were made in the build process and the powder was enclosed directly. On the other hand, powder samples were taken after the process with a specially made sampler (Bürkle GmbH, Bad Bellingen, Germany) consisting of a multi-part, double-walled rotatable tube construction (Fig. 1). By arranging three chambers one above the other, three sample volumes of approx. 28g each can be taken simultaneously at different heights at the same build platform position.

For each powder the information provided by the powder manufacturer such as powder batch, fraction and material, as well as the sampling time, the number of construction jobs carried out, machine information and any additional information such as the condition (sieved, unsieved) was logged. This metadata is recorded sample-specifically in a database, the so called powder information management system (PIMS). At the time of writing, approx. 100 powder samples are available for characterization.

Fig. 1. Picture of the special powder sampler.

2.2. Powder sample characterization

The properties considered and the characterization methods for the acquisition of the powder properties are the determination of the particle morphology via Dynamic image analysis with Camsizer X2 (Retsch Microtrac, Germany, Haan) and the assessment of the chemical composition via EDS and oxidation with carrier hot gas extraction (Inductar EL, Elementar Analysensysteme GmbH, Langenselbold, Germany). These properties have a significant influence on the rheology of the powders. Therefore, the rheology in the matter of the flow rate and the shear properties was also measured via a FT4-Powder-rheometer from Freemantech (Tewkesbury, UK).

Especially the application of the dynamic image analysis with the Camsizer X2 enables a comprehensive determination of morphological parameters of the powder compared to other methods like the more established laser diffraction spectroscopy. Besides the characteristic particle diameter quantile d10, d50 and d90, also other shape parameters like the sphericity (SPHT3), symmetry and particle aspect ratio can be measured.

All data obtained from the powder reference measurements as well as the meta data of the powders was saved in a special database of powder properties (PIMS, see chapter 2.5) designed with interfaces for data export and visualization.

Only the morphological powder properties (d10, d50, d90 and spht3) were considered for further analysis. For the other powder properties, there were still no or only very few differences between the powder materials, or not enough measurements were carried out yet. However, these properties will also be included in the investigation in the future.

2.3. Hyperspectral imaging

The hyperspectral measurement of the powders is performed with two different pushbroom HSI measuring systems with a diffuse halogen illumination. A schematic representation of the system is shown in Fig. 2. The system is equipped with a VNIR HSI camera (Hyperspec-VNIR, Headwall Photonics Inc., Bolton, MA, USA). The VNIR camera is equipped with an EMCCD detector with 1004 × 1002 pixels (Luca R 604, Andor Technology Ltd., Belfast, UK) with a wavelength range between 400 nm and 1000 nm. The two used systems differ in terms of the lens used. One system, called VNIR-HSI from here on, is equipped with a Xenoplan 23 mm f/1.4 lens (Jos. Schneider Optische Werke, Bad Kreuznach, Germany). The other system, called mVNIR-HSI, is equipped with a telecentric lens with fixed working distance of 86 mm (S5LPJ2426, Sill Optics, Germany). The main difference between the two systems is therefore the FOV and thus the spatial resolution of the measurements.

The lighting for the measurement is provided by 6 halogen lamps with a power of 25 W each. The diffuse illumination of the samples is done by an integration tube made of Spectralon (Labsphere Inc., North Sutton, NH, USA). The movement of the samples is controlled by a linear stage (VT 80, PI Micos, Eschbach, Germany). The integration and the control of the system components, as well as and the data acquisition is carried out by the dedicated HSI software suite imanto®pro (Fraunhofer IWS, Dresden, Germany).

To avoid irregularities in the lighting and to eliminate the influence of dark current, a white and a dark correction for each wavelength according to Eq. 1 was carried out.

$$I_c(\lambda) = \frac{I_o(\lambda) - I_d(\lambda)}{I_w(\lambda) - I_d(\lambda)} \quad (1)$$

I_c is the corrected image and I_o the original image for the wavelength λ. I_d is the dark signal recorded with the light source switched off and the lens covered, and I_w is the white reference. For the white reference (I_w), a Spectralon plate was recorded under the same measuring conditions as the original image.

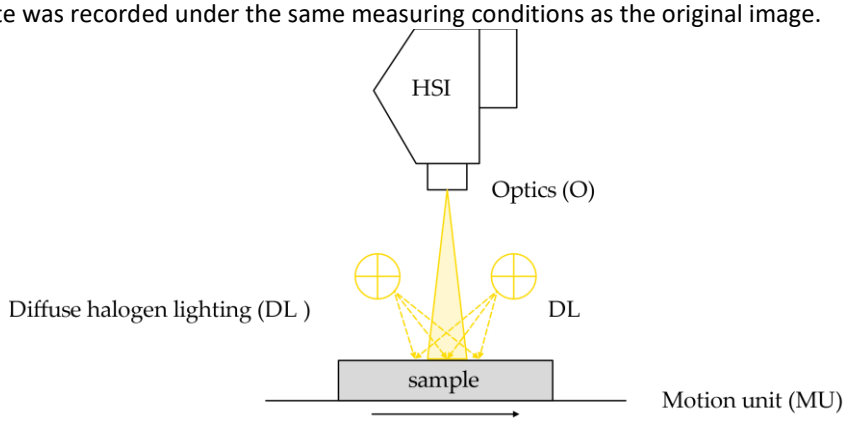

Fig. 2. Schematic representation of the hyperspectral imaging system. HSI: VNIR or NIR HSI camera. O: optics of the HSI camera. DL: diffuse halogen lighting. MU: motion unit.

Each powder sample was measured with both HSI systems. Two measurements were made per sample using the VNIR-HSI system and three measurements were made using the mVNIR-HSI system. For the measurements, the metal powder was placed in a sample holder. This is a metal plate with a 50 x 50 x 5 mm cavity into which the powder can be filled (see Fig. 3). Before the measurement, the powder was smoothed with a silicone lip, similar to the process that takes place in an LPBF system.

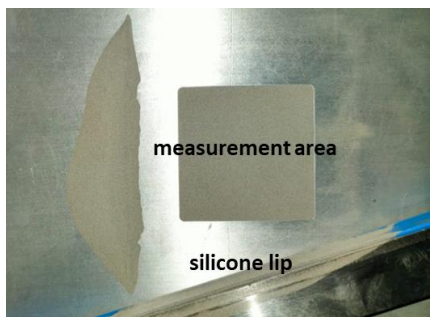

Fig. 3. Picture of the sample holder with powder and silicone lip.

For the VNIR-HSI system the measurements were performed with a working distance of 250 mm, an exposure time of 7 ms, a recording frequency of 40 Hz and 4× binning in the spectral dimension. This results in a field of view (FOV) of ~ 90 mm, a lateral pixel resolution of ~ 90 µm, and a spectral resolution of ~ 3 nm. For the mVNIR-HSI system the measurements were performed with a working distance of 86 mm, an exposure time of 30 ms, a recording frequency of 20 Hz and 4× binning in the spectral dimension. This results in a FOV of ~ 5 mm, a lateral pixel resolution of ~ 5 µm, and a spectral resolution of ~ 3 nm. For both systems the advance speed of the sample was set to obtain square pixels and therefore the same spatial resolution in both directions. The result of each measurement was a hypercube with 191 spectral bands between 400 nm and 1000 nm for both systems. The spatial size of the hypercubes is 400 x 400 pixel for the VNIR and 1000x1000 pixel for the mVNIR measurement. Figure 4 shows example measurements of a new and an often used Inconel718 powder measured with the VNIR- and the mVNIR-HSI system respectively. It is apparent that there are differences between the new and the used powder in the texture of the measurements as well as in the mean spectra.

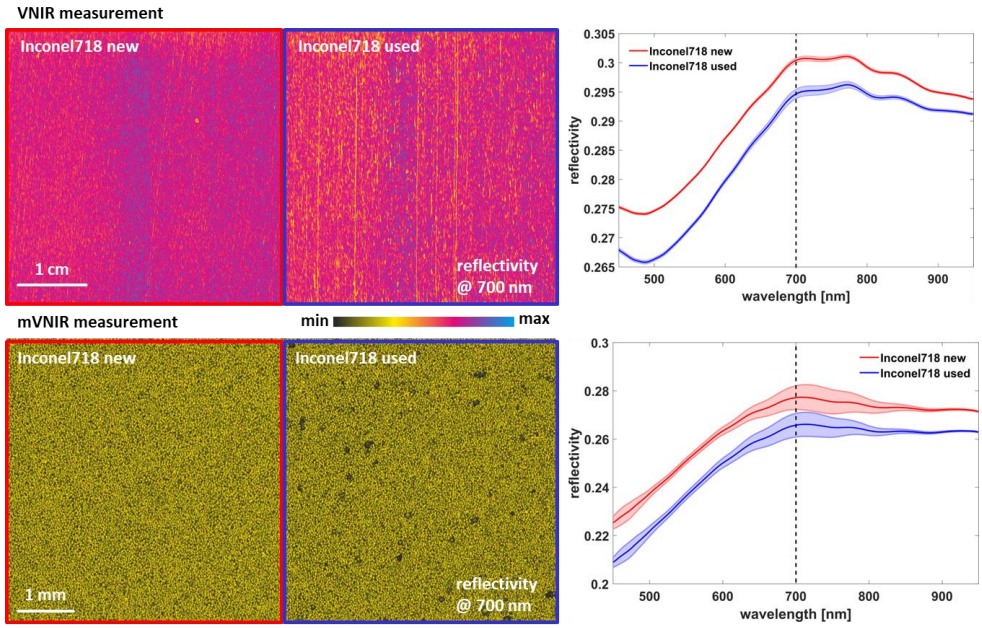

Fig. 4. Examples of hyperspectral measurements with the VNIR-HSI setup (top) and the mVNIR-HSI setup (bottom) of a new and an often used Inconel718 powder and the mean spectra and the variance of the measured area. The images on the left show the colour coded reflectivity at a wavelength of 700 nm.

2.4. Data evaluation and model training

For each powder measurement a data set of 30.5 million (VNIR measurement) respectively 191 million (for the mVNIR measurement) data points was recorded. This data cannot be used directly to train machine learning models, because of the high redundancy of the data. Therefore, the first step in data evaluation is to compress the data. Therefore, the spectral information and the texture information of the hyperspectral measurements are considered independently of each other. To determine the spectral information, the mean spectrum is calculated for each hypercube. To determine the texture information, the wavelength image at which the hyperspectral measurement has the greatest sharpness was determined first. This was accomplished selecting the wavelength image with the highest mean variance in the spectral range from 500 nm to 800 nm.

To compress the textural information of the grayscale images further, two methods were used: rotational invariant local binary patterns (LBP, (Bouwmans et al. 2016)) and the discrete wavelet transform (DWT, (Mallat 1989)). For the LBP different values for the neighbour points p and the spatial resolution r were used. For the DWT the level of decomposition l and the used wavelet were also varied. The optimal values for those values were selected automatically using hyperparameter optimization. To vectorise the results of the DWT decomposition, for each image of detail coefficients the mean, the variance and the Shannon entropy H(x) was calculated according to Eq. 2:

$$H(x) = -\sum_{i=1}^{n} p_i \log_2 p_i \tag{2}$$

Where pi is the occurrence probability of a certain value of the detail coefficients.

To further unify and structure the spectral and texture data, a principal component analysis (PCA) was also performed before the training of the machine learning algorithms. The optimal number of principal components was again determined by hyperparameter optimization.

The compressed spectral and textural data for each hypercube was then used as input data for the machine learning models. The goal of these models is to classify different powder types and batches, as well as to predict the powder size (d10, d50 and d90) and the sphericity (spht3) from the hyperspectral measurements. The algorithm used depends on the type of target variable. For the discrete target variables powder type and powder batch (classification problems), logistic regression (LR, (Hosmer und Lemeshow 2087)) was used. For the continuous target variables d10, d50, d90 and spht3 (regression problems), ElasticNet (EN, (Zou und Hastie 2005)) regression was used. For the hyperparameter optimization and the validation of the models 5fold nested cross-validation was used. Each model was trained tree times to minimize random variations.

The hyperparameter optimization was performed using random search (RS, (Bergstra und Bengio 2012)) over 30 runs. This means that the hyperparameters of the algorithms were randomly varied thirty times and the best model was selected. A hyperparameter is a parameter whose value is used to control a machine learning model and can have a large influence on the model performance. The considered hyperparameters are shown in Table A. 1. To compare the obtained models the RMSE and R^2 for the regression models respectively the balanced accuracy for the classification models were calculated and compared.

The RMSE is the root mean squared error and is calculated using Eq. 3:

$$\mathrm{RMSE} = \sqrt{\frac{\sum_{i=1}^{n}(\hat{y}_i - y_i)}{n}} \tag{3}$$

Where ŷ and y are the true and the predicted target values and n is the number of target values.

The balanced accuracy is calculated using Eg.4:

$$Acc = \frac{TPR + TNR}{2} \tag{4}$$

Where TPR is the true positive rate and TNR is the true negative rate of the classification.

The training was done for the VNIR and the mVNIR data separately. For each target variable (powder typ, powder batch, d10, d50, d90 and spht3) four models using different datasets were trained:

- only using the spectral features (**spec**)
- only using the LBP features (**LBP**)
- only using the DWT features (**DWT**)
- and using all features (**all**)

To use **all** features for training, the results of the PCAs for the spec, the DWT and the LBP data were combined to one feature vector and used as input data to train the machine learning models.

2.5. Powder Information Management System

The hyperspectral measurements and the ground truth reference data of the powders were stored in a central database, the powder information management system (PIMS). Data integration is a crucial issue in the environments of heterogeneous material characterization data. The PIMS presents a database architecture which implements knowledge discovery from the data process. The solution allows the integration of any data sources and implementation of analytical methods in one database environment. User might track and manage sub database (samples, devices, probes, materials, stock, projects, image

repositories, sensors) and link, cross-search their results (raw data) between those databases. Once data is ready to be pulled out of the system, there are easily accessible and configurable reports and exports to statistical and machine, deep learning software applications. The PIMS as an image database is a cloud-hosted with data entry performed on a web-based interface.

3. Results and discussion

3.1. Powder sample overview and measured properties

A total of 100 powder samples were characterized using the methods described in chapter 2.2 to obtain ground truth values for the HSI measurements. The characterization was limited to the morphological parameters of the powders: the size distribution d10, d50 and d90, the spherizity as well as the symmetry and the aspect ratio of the powders. To visualize the results of the morphological characterization of the powders, principal component analysis (PCA) was performed on the results received. The results of the PCA show that it is possible to distinguish the 316L and the Inconel718 powders based on their morphological properties (see Fig. 5). The differences between the different Inconel718 powder batches and the sieved and unsieved powders are less pronounced but visible. In summary, the mophological differences within a powder material are much less pronounced than the differences between the powder materials 316L and Inconel718.

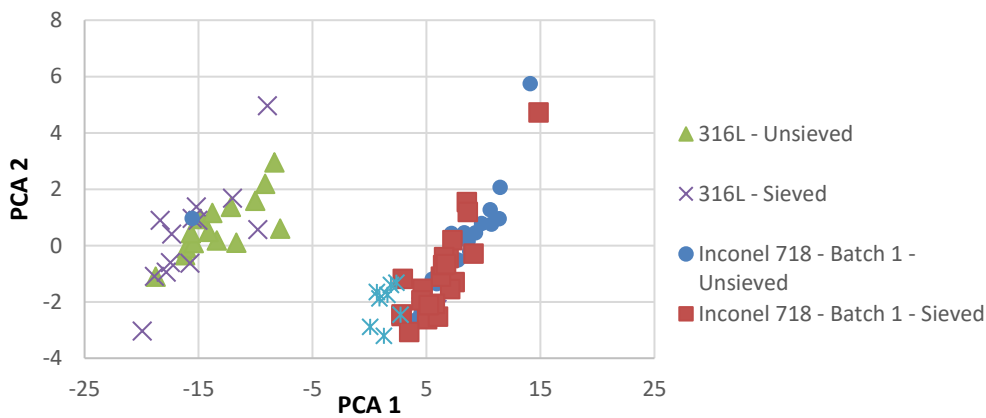

Fig. 5. Principal Component Analysis of the morphological properties

3.2. Results of modeling using machine learning

3.2.1. Classification of powder type

In a first step, it was studied whether it is possible to distinguish different powder materials on the basis of hyperspectral measurements and which features (spectra, texture) are best suited for this purpose. For the investigations, the powder materials Inconel718 (Ni alloy) and 316L (stainless steel) were considered. The powders investigated come from different processing cycles, and the Inconel718 powders are powders from two different batches. Table 1 shows the balanced accuracy for the cross validation of the optimized classification models and

VNIR mVNIR

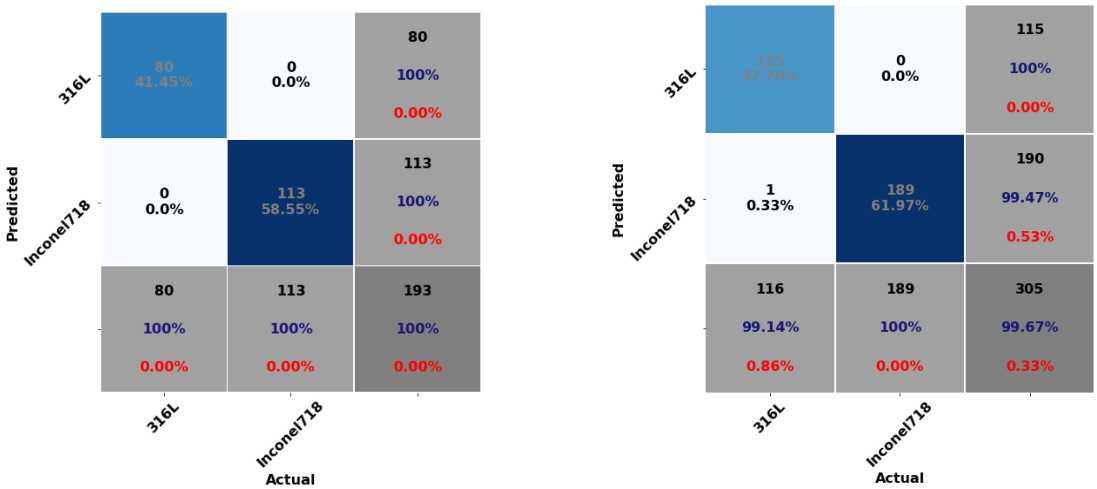

Fig. **6** shows the confusion matrix for the best found model for the VNIR and the mVNIR data respectively.

The best accuracies are obtained for both the VNIR measurements and the mVNIR measurements for the **spec** data and are 100 % and 99.6 % respectively. It is therefore possible to predict the material of the powders on the basis of their spectral properties. If the texture is considered, the accuracy of the prediction is lower and a more differentiated picture is observed. For the **LBP** data, especially for the VNIR measurements, only a relatively low accuracy of 68 % is achieved. For the mVNIR measurement, the accuracy increases to 90.5 %. This can be explained by the significantly higher spatial resolution and thus the higher information content of the mVNIR measurements. For the **DWT** data, a relatively good accuracy of 96.4 % (VNIR) and 98.8 % (mVNIR) can be achieved for both measurements. The results show that the powders can also be distinguished by their texture and that it is therefore possible to predict the powder material using the texture. Furthermore, the **DWT** method is shown to be more suitable for the parameterization of these differences. If the entire data is used for classification (**all**), the accuracy of the prediction is reduced slightly. The reason for this is the higher number of features that are included in the model training. This increases the dimensionality of the problem, which can lead to an increased overfitting of the trained models. As a result, these models achieve a lower accuracy in the prediction, which decreases the accuracy of the cross-validation.

Table 1. Mean balanced accuracy for the cross validation of the best found classification models for the prediction of the powder type. The best accuracy is underlined. The standard deviation of the accuracy was omitted for clarity.

data	Acc(VNIR) [%]	Acc(mVNIR) [%]
spec	<u>100.0</u>	99.6
LBP	68.0	90.5
DWT	96.4	98.8
all	99.9	99.3

VNIR mVNIR

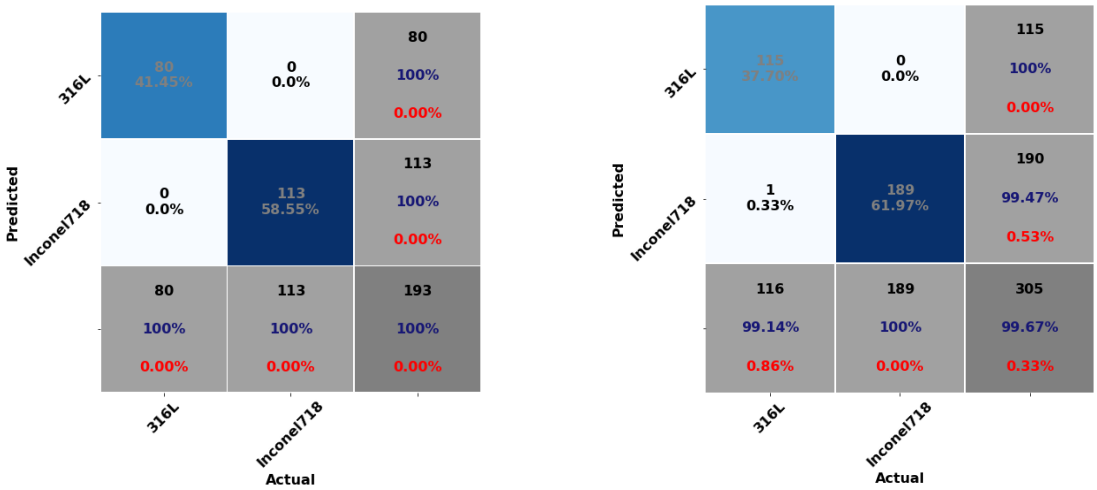

Fig. 6. Confusion matrices for the best found classification models for the prediction of the powder type for the VNIR (left) and the mVNIR (right) measurements.

3.2.2. Classification of powder batch

After the successful classification of the powders investigated with regard to the powder material, the next step is to investigate whether it is also possible to distinguish between different powder batches of the same powder material. For this analysis, only the Inconel718 powders were considered, of which 50 samples belong to one batch (batch 1) and 20 samples to another batch (batch 2).

Table 2 shows the mean balanced accuracy for the cross validation of the optimized classification models and

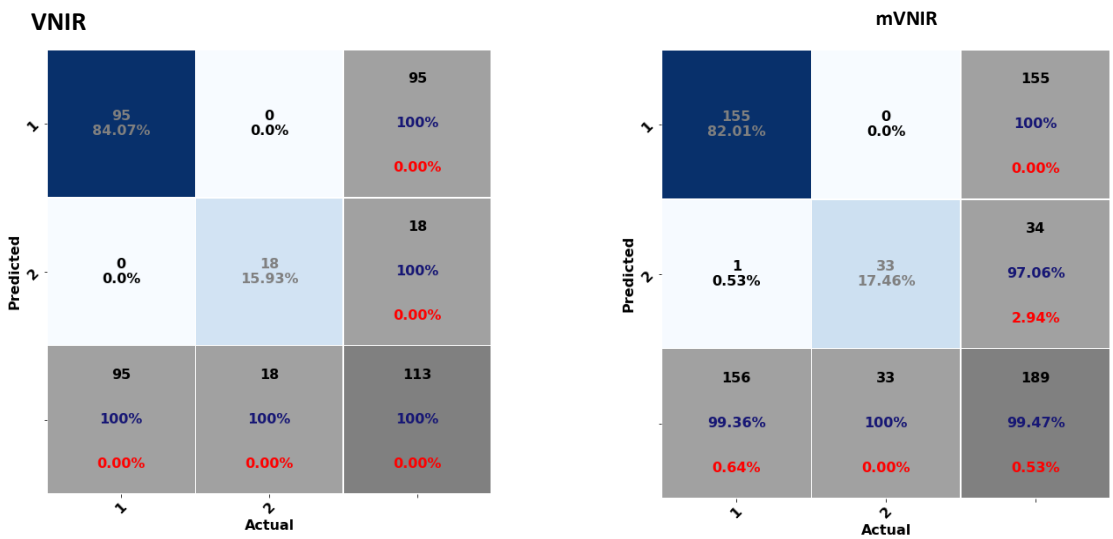

Fig. **7** shows the confusion matrix for the best found model for the VNIR and the mVNIR data respectively. The results are very similar to those obtained for the prediction of the powder material. With the spectral data (**spec**), a prediction of the powder batch is possible with an accuracy of about 100% for both the VNIR

and the mVNIR measurements. When using the texture data of the measurements, the accuracy is reduced to 90.1 % (VNIR, **DWT**) and 96.2 % (mVNIR, **DWT**), but is still in a promising range. Again, better classification accuracies are obtained with the **DWT** data compared to the **LBP** data.

It can therefore be concluded that the powders of the two Inconel718 batches under investigation differ in terms of both their spectral and their texture properties, and that classification is therefore possible on the basis of the hyperspectral measurements.

Table 2. Mean balanced accuracy for the cross validation of the best found classification models for the predicition of the powder type. The best accuracy is underlined. The standard deviation of the accuracy was omitted for clarity.

data	Acc(VNIR) [%]	Acc(mVNIR) [%]
spec	<u>100.0</u>	99.9
LBP	77.9	96.0
DWT	90.1	96.2
all	<u>100.0</u>	99.9

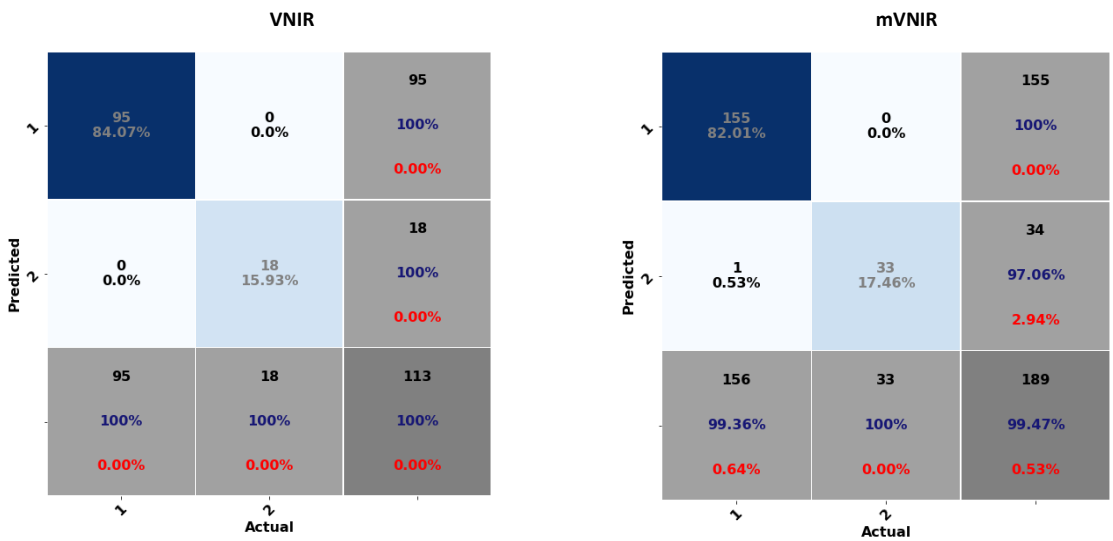

Fig. 7. Confusion matrices for the best found classification models for the prediction of the powder batch for the VNIR (left) and the mVNIR (right) measurements. 1: Batch 1. 2: Batch 2.

3.2.3. Prediction of the powder size

After demonstrating that it is possible to qualitatively distinguish powders in regard to their material and to differentiate between powder batches using hyperspectral measurements, the next step is to try to quantitatively predict properties of the powders. First, the size distribution of the powders, expressed by the values d10, d50, and d90, is considered.

Table 3 shows the mean RMSECV for the cross validation of the optimized regression models and Fig. 8 shows the regression plot for the best found model for the VNIR and the mVNIR data respectively. It can be seen that lower RMSECV values are obtained for the mVNIR data than for the VNIR data, which can be explained by the significantly higher spatial resolution of these measurements. At around 5 µm, the

resolution is within the range of the actual size of the powder particles. The best RMSECV values are obtained with 0.577 (d10), 0.814 (d50) and 0.851 (d90) using all data (**all**), which shows that for the prediction of the powder size distribution both the spectral and the texture information of the hyperspectral measurements are needed. The regression plot (Fig. 8, right) shows a clear correlation of the measured and predicted d10 values (R2 = 0.65). This is also reflected in the fact that relatively similar RMSECV values are obtained when considering the different data sets (**spec**, **LBP** and **DWT**) separately. Furthermore, it can be seen that the RMSECV values increase from d10 to d90, which can be explained by the increase in the range of values for each parameter, which leads to higher RMSE values, even if the model has the same quality.

The results for the VNIR data are significantly worse especially when the texture features (**LBP** and **DWT**) are considered. This shows that the regression here is mainly based on the fact that the powder samples considered (Inconel718 and 316L) differ in terms of their size distribution (see chapter 3.1). The regression model therefore mainly recognizes these two powder types (as already shown in chapter 3.2.1), which are correlated with the size distribution. A real prediction of the powder size from the hyperspectral measurements therefore does not seem to be possible. This is also indicated by the regression plot (Fig. 8, left), which shows no clear correlation between the measured and predicted d10 values (R2 = 0.59) and a clustering of the powder materials.

In summary, there is a correlation of the mVNIR measurements to the size distribution of the powders considered and therefore the size distribution can be predicted from the mVNIR measurements with relatively low error. The high spatial resolution of the measurements seems to be crucial for the prediction, since no good correlation to the size distribution is obtained for the VNIR data. The spectral information also seems to be correlated with the size distribution, but there is probably a co-correlation between powder type, powder size distribution and the spectral reflectance of the powders. For a more detailed investigation, more powders from different materials and with different size distributions need to be studied.

Table 3. Mean RMSE for the cross validation of the best found regression models for the prediction of the powder size d10, d50 and d90. The best RMSE for each parameter is underlined. The standard deviation of the accuracy was omitted for clarity.

	RMSE(VNIR)			RMSE(mVNIR)		
data	d10	d50	d90	d10	d50	d90
spec	0.654	0.905	1.1695	0.662	0.815	1.229
LBP	1.552	1.451	1.280	0.763	0.894	0.957
DWT	1.066	1.175	1.343	0.712	0.867	1.038
all	0.680	0.928	1.099	<u>0.577</u>	<u>0.814</u>	<u>0.851</u>

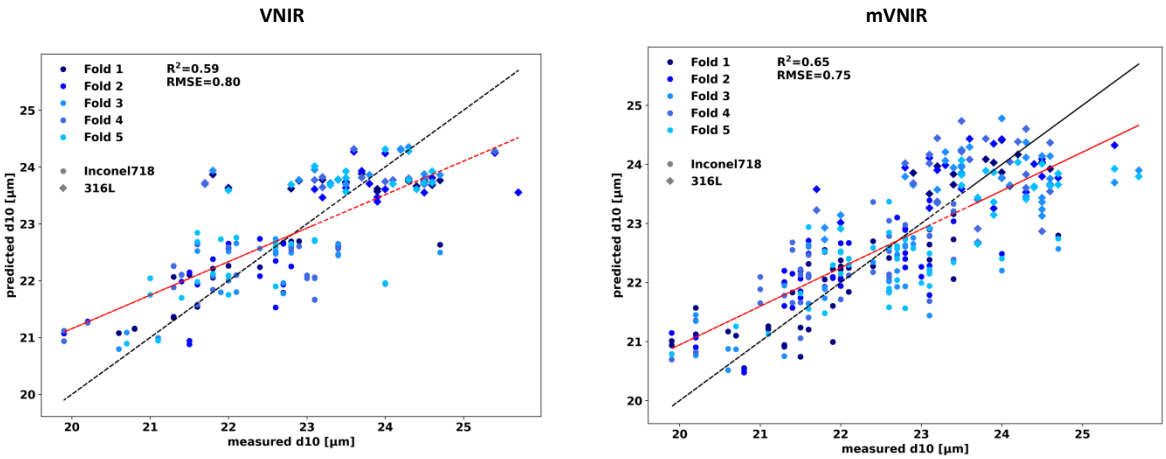

Fig. 8. Regression plots for the best found models for the prediction of the powder size d10 for the VNIR (left) and the mVNIR (right) measurements. The plots for d50 and d90 show a similar behaviour.

3.2.4. Prediction of the powder sphericity

The last aspect that was investigated is the prediction of the sphericity of the powder material from the hyperspectral measurements. As shown in chapter 3.1, there is a clear difference in sphericity between the Inconel718 and 316L powders. It can therefore also be assumed here that there is a co-correlation between powder material, reflectivity and sphericity and that the results obtained can only be used to a somewhat limited extent. However, there are a small number of 316L powders whose sphericity is in the range of the Inconel718 powders. If the sphericity of these powders can be predicted well, this indicates that direct prediction of sphericity from the HSI data is possible.

The results show that the best prediction results are again obtained using all data (**all**). This is true for both the VNIR and the mVNIR data. The RMSE values for the mVNIR data are slightly better for the VNIR data (0.259 vs. 0.236). But the regression plots show that there is clustering of the powder materials for the VNIR data (Fig. 9, left). The 316L powders with low sphericity are not predicted correctly and have a large prediction error. For the mVNIR data (Fig. 9, left), however, the sphericity of these powder samples is predicted better and the prediction error is smaller.

Thus, for both data sets, there is a correlation between HSI measurements and the sphericity of the powders, which seems to be in part caused by the co-correlation of powder material and sphericity. In the mVNIR data, however, there also appears to be an actual correlation between HSI measurements and sphericity. Again, more powders from different materials and with different sphericity should be investigated to validate the results.

Table 4. Mean RMSE for the cross validation of the best found regression models for the predicition of the powder sphericity spht3. The best RMSE is underlined. The standard deviation of the accuracy was omitted for clarity.

data	RMSE(VNIR) $*10^{-4}$	RMSE(mVNIR) $*10^{-4}$
spec	0.267	0.270
LBP	1.197	0.360
DWT	0.489	0.320
all	<u>0.259</u>	<u>0.236</u>

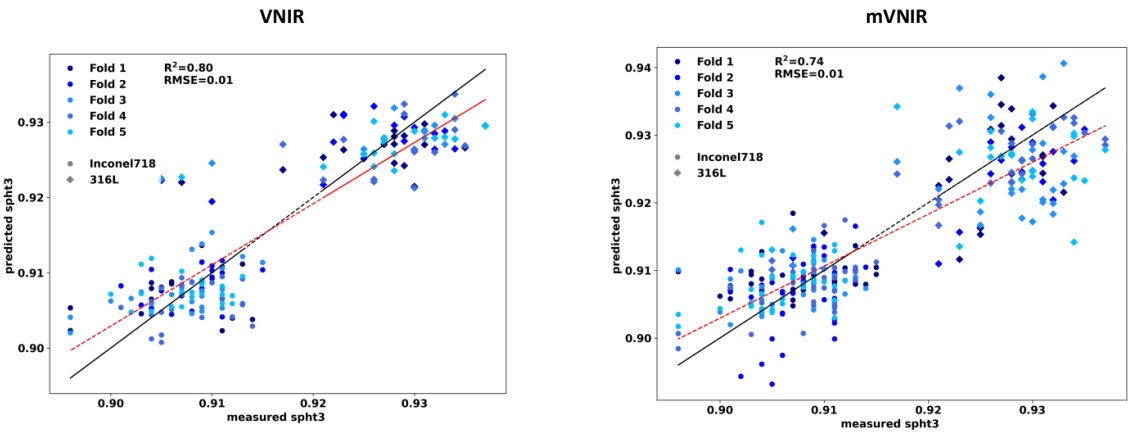

Fig. 9. Regression plots for the best found models for the prediction of the powder sphericity spht3 for the VNIR (left) and the mVNIR (right) measurements.

4. Conclusion and Outlook

In this work, the use of hyperspectral imaging in the VNIR spectral range for the fast, non-contact and inline-capable characterization of metal powders from AM was demonstrated. It was shown that it is possible to distinguish different powder types (316L and Inconel718) as well as powders of different batches (Inconel718) with very high accuracies. Furthermore, it is possible to predict certain morphological properties of the powder samples on the basis of the hyperspectral measurements. This could be shown for the size distribution (d10, d50 and d90) as well as for the sphericity of the powder particles. It was shown that both the spectral properties and the texture of the powders investigated are correlated with the powder properties. In addition, better results tended to be obtained with the high-resolution HSI measurements. In the future, the robustness and the applicability of the prediction models to other puvler materials will be investigated. In addition, attempts will be made to predict other properties such as the rheology and the chemical properties of the powders.

In the future, the developed method could be used in the series production of powder-based AM processes. In these processes, usually only one powder is used, and the HSI-based powder characterization could enable continuous monitoring of the powder quality. For example, differences between powder batches from different manufacturers or degradation of powder properties during production could be detected without the need for time-consuming and labor-intensive atline powder quality checks. In the long

term, the method could also be used to control the AM process, for example to adapt the process parameters to the properties of the used powder. In further development steps the capabilities of the HSI can also be used for in-situ measurements of the powder bed quality in powder bed processes with respect to segregation and contamination.

Acknowledgements

The authors acknowledge the financial support by the Federal Ministry of Education and Research of Germany in the framework of Agent3D (project number 03ZZ0230).

References

Bergstra, James; Bengio, Yoshua (2012): Random search for hyper-parameter optimization. In: Journal of Machine Learning Research 13 (Feb), 281--305.

Bouwmans, Thierry; Silva, Caroline; Marghes, Cristina; Zitouni, Mohammed Sami; Bhaskar, Harish; Frelicot, Carl (2016): On the Role and the Importance of Features for Background Modeling and Foreground Detection. http://arxiv.org/pdf/1611.09099v1.

Hosmer, David W.; Lemeshow, Stanley (2087): Applied Logistic Regression. Hoboken: John Wiley & Sons. http://gbv.eblib.com/patron/FullRecord.aspx?p=3056835.

Linaschke, Dorit; Gruber, Florian; Stepien, Lukas; Lopez, Elena; Brueckner, Frank; Leyens, C. (2019): Powder Material Analysis by Hyperspectral Imaging.

Mallat, S. G. (1989): A theory for multiresolution signal decomposition: the wavelet representation. In: IEEE Trans. Pattern Anal. Machine Intell. 11 (7), S. 674–693. DOI: 10.1109/34.192463.

Steven, M.; Dörseln, J. N.; Pollmeier, I.; Schade, S.; Stetzka, R. M.; Gerhard, D. et al. (2020): Smart Factory: Einsatzfaktoren - Technologie - Produkte: KOHLHAMMER Verlag. https://books.google.de/books?id=z4l8zQEACAAJ.

Zou, Hui; Hastie, Trevor (2005): Regularization and variable selection via the elastic net. In: J Royal Statistical Soc B 67 (2), S. 301–320. DOI: 10.1111/j.1467-9868.2005.00503.x.

Appendix A. Optimized Hyperparameters for machine learning models

Table A. 1. Optimized hyperparameters and optimization range.

Algorithm / preprocessing step	parameter	range
spec	normalization	L1, L2, SNV
	PCs for PCA	2 - 8
LBP	radius r	3, 7, 11, 15
	points p	8, 24
	PCs for PCA	2 - 4
DWT	wavelt	db1, db4, sym2, sym4, coif1, coif3, bior3.5
	decomposition levels	2, 4
	PCs for PCA	2 - 4
Logistic Regression	Solver	newton-cg, lbfgs, saga
	C	10^{-2} - 10^{2}
Elastic Net	α	10^{-5} - 10^{3}
	L1 ratio	0 - 1